2

X-625-72-129

PREPRINT

NASA TM X-65891

METALLIC IONS IN THE EQUATORIAL IONOSPHERE

A. C. AIKIN

R. A. GOLDBERG

MAY 1972

GSFC

GODDARD SPACE FLIGHT CENTER

GREENBELT, MARYLAND

METALLIC IONS IN THE EQUATORIAL IONOSPHERE

by

A. C. Aikin
R. A. Goldberg
Laboratory for Planetary Atmospheres
NASA/Goddard Space Flight Center
Greenbelt, Maryland

ABSTRACT

Four positive ion composition measurements of the equatorial E region at Thumba, India are presented. During the day, the major ions between 90 and 125 km are NO^+ and O_2^+. The relative concentrations are similar to those observed at midlatitudes but exhibit unusual structural behavior with altitude. A metallic ion layer centered at 92 km is observed, and found to contain Mg^+, Fe^+, Ca^+, K^+, Al^+, and Na^+ ions. The layer is explained in terms of a similarly shaped altitude distribution of neutral atoms which are photoionized and charge exchanged with NO^+ and O_2^+. Three body reactions form molecular metallic ions which are rapidly lost by dissociative ion-electron recombination. Unfortunately reactions which create molecular ions from Na^+ and K^+ using CO_2 as a third body to form cluster ions are too slow to account for the observed alkalai metal ion distribution.

Nighttime observations show downward drifting of the metallic ion layer caused by equatorial dynamo effects. These ions react and form neutral metals which charge exchange with NO^+ and O_2^+ to produce an observed depletion of NO^+ and O_2^+ within the metallic ion region. The inclusion of drift effects is found to be necessary in producing a proper description of metal ion behavior at the magnetic equator. Similar considerations are probably appropriate at other latitudes.

INTRODUCTION

It is essential for the understanding of the equatorial ionosphere and electrojet to have a detailed knowledge of the altitude and temporal variation of the positive ion species and concentrations. Several rocket flights have aided in defining the equatorial E region electron density distribution (Aikin and Blumle, 1968); however, prior to the work reported here, no measurements had been made of the ion composition in this region. This paper gives the results of two daytime and two nighttime measurements of the ion composition and electron density of the E region at the magnetic equator, using rocket payloads launched from the Thumba Equatorial Rocket Launch Site (dip latitude, 0.85^{o}S).

Under most circumstances the major ionic constituents in the E region are observed to be NO^{+} and O_2^{+}. The measured distribution of these molecular ions can be compared with theoretical profiles based on a photochemical model such as that of Keneshea et al, (1970). At night we observe that below 100 km the ions NO^{+} and O_2^{+} are sufficiently depleted to permit metallic atomic ions to become the major ionic constituents.

Metal ions are considered to be a permanent feature of the lower E region and have been observed over a large

range of latitudes and times (e.g. Istomin, 1963; Narcisi, 1968). Because of several factors their distribution is difficult to explain. The metal ions result in part from the photoionization of neutral metals and charge exchange between neutral metals and the principal ions of the E region, NO^+ and O_2^+. The distribution of neutral metals varies seasonally and geographically in an ill-defined manner (Hunten, 1964). The reactions and rate coefficients for the interaction of metal ions with neutrals are very uncertain (Ferguson, 1972). Because metal ions are atomic and thus have lifetimes of order 10^5 times that of molecular ions, they are more subject to dynamical effects. For example, at midlatitudes metallic ions are found in sporadic E layers (E_s) formed by interaction of wind shears with the vertical component of the terrestrial magnetic field (Whitehead, 1961). Electric field induced vertical motion of such a metal ion layer at temperate latitudes has been treated by Chimonas and Axford (1968).

At the geomagnetic equator, dynamo effects induce vertical drifting of the ionospheric plasma. The diurnal variation of the dynamo electric field and its relation to the F region has been detailed by measurements at Jicamarica, Peru (Balsley, 1969 a, b; Balsley and Woodman 1969). Based on ionograms a similar behavior is deduced

for Thumba. The rocket observations show that the distribution of metal ions in the E region is also affected by this electric field. This paper presents measured evidence for equatorial electric field modification of the metal ion distribution. The behavior of all species are discussed although large uncertainties in rate coefficients, source and loss functions of the neutral distribution, and other parameters which determine the metallic ion structure limit the accuracy of the quantitative results. These results have important implications for the metal ion distribution at mid-latitudes.

INSTRUMENTATION

Information pertinent to the four rocket firings is listed in Table I. Each payload contained a quadrupole ion mass spectrometer housed in a titanium getter pumped system assisted by two triode ion pumps for inert gas pumping (Goldberg and Blumle, 1970). The details of this system plus the daytime performance characteristics are described in Goldberg and Aikin (1971). The nighttime details will be discussed elsewhere.

The daytime flights also contained radiowave absorption experiments operated at 1.865 and 3.030 MHz to determine electron density, and Gerdien probes for total positive ion density (Aikin et al, 1972). The electron density profiles at night were determined by continuous wave dispersive Doppler experiments (Seddon, 1953; Bauer and Jackson, 1962; Jackson, 1971) operated at frequencies of 73.6 and

24.53 MHz. Electron density profiles determined by the above techniques were used to normalize the spectrometer currents to absolute values. Free molecular flow effects were taken into account in obtaining the correct relative ion densities.

All rocket trajectories were determined using a tone range/telemetry interferometer tracking system developed by Hudgins and Lease (1969).

Figure 1 illustrates typical spectra observed at two altitudes, 89 km and 148 km, for nighttime conditions at the magnetic equator. The mass range swept is 1 to 41 amu. Two high pass filter modes were also employed to deduce the total ion density > 41 amu. These are shown in the figure for the ranges $1 \rightarrow \infty$ and $32 \rightarrow \infty$ amu. The use of two mass ranges in the high pass filter mode permits inflight calibration of the high pass filter mode data as outlined in Goldberg and Aikin (1971). The measured ionic constituents and their identification are 30^+, NO^+; 32^+, O_2^+; 28^+, N_2^+; and 16^+, O^+; which are gaseous ions resulting from ionization of the principal gases of the thermosphere. In addition, we identify the metallic ions 23^+, Na^+; 24^+, Mg^+; 27^+, Al^+; 28^+, Si^+; 39^+, K^+; 40^+, Ca^+; and 56^+, Fe^+; the last from high pass filter mode data during the nighttime flights. Since the nighttime high pass filter mode data is known to contain a fractional contribution from $O_2^+(32^+)$, the Fe^+ deduced from this data must be considered an upper quantitative limit. We note

that 28^+ can either be N_2^+ or Si^+, with no apparent method of separating the two at this time.

THE DISTRIBUTION OF NO^+ AND O_2^+

The distribution of the major ionic constituents, as illustrated in Figure 2 for the daytime equatorial E region, is characterized principally by NO^+ and O_2^+. The presence of the equatorial electrojet, which is centered near 109 km (Maynard and Cahill, 1965), has no apparent effect on the ion composition. Above 95 km the major ionic constituents exhibit an unexplained oscillation that slowly dampens in amplitude and wavelength. No such behavior is apparent in the nighttime data shown in Figure 3, but here the height resolution is greatly reduced because of the greater velocity of the rocket.

The NO^+/O_2^+ ratio for the four flights is shown in Figures 4 and 5 for daytime and nighttime, respectively. There have been few previous measurements of this ratio below 100 km. The data of Narcisi (1968) for a zenith angle of 49° showed that between 95 and 115 km the NO^+/O_2^+ ratio was less than unity. None of our daytime data exhibits a ratio less than unity for any extended altitude. For a zenith angle of 27.8° we find NO^+/O_2^+ ratios of about 2 for the altitude range 100 to 125 km. Our results are well within the predicted values as deduced by Danilov (1972).

At night the ratio ranges between 5 and 150 over the entire altitude region. Narcisi et al, (1967) give

a ratio of 15 $\pm$ 2 for 95 to 103 km at midnight. Our comparable measurement is at 1:08 LMT and a ratio ranging between 45 and 150 is obtained.

Keneshea et al. (1970) have conducted a complete diurnal study and their computed results are shown in Figures 4 and 5. We have performed a similar computation and our daytime results are shown for comparison in Figure 4. The agreement of our model is better with the observed daytime data because of the larger calculated ratio for NO^+/O_2^+. The difference between the two computations is caused in part by the difference in values of the rate coefficient k_1 for the reaction $O_2^+ + NO \rightarrow NO^+ + O_2$ (6×10^{-10} for Keneshea et al, vs 7.7×10^{-10} cm^3 sec^{-1} for our calculation) and by the use of a larger value for neutral NO above 100 km.

The NO^+/O_2^+ ratio is a sensitive function of the solar flux, since this factor also enters into the equation through the electron density, N_e. There is considerable uncertainity in the solar X-ray flux in the 30 to 60 A range. This is particularly true of the 30 to 40 A interval which includes the strong CVI line at 33.6 A and which Bourdeau et al (1965) noted was an important ionization source in the 90 to 100 km altitude region. Values for the measured flux at 33.6 A range from 2-3 $\times 10^{-3}$ ergs/cm^2sec (Manson, 1967, 1968) to 6×10^{-2} ergs/cm^2 sec (Argo et al, 1970). Earlier computations of an E region model used 3×10^{-3} ergs/cm^2 sec (Keneshea, 1967). For the Keneshea et al, (1970) model it was found necessary to increase the flux in the 30 to 60 A

range by a factor of 4 over the earlier computation. Our computations employ a flux in this spectral range which is a factor of 2 less than the Keneshea et al,(1970) values. The measured X-ray flux in the 1-8 A band was enhanced at the time of the daytime flights (Aikin et al, 1972). No measured data were available concerning the 30 to 60 A flux. The Meira (1971) nitric oxide profile, which is utilized in our computations, leads to unacceptably large values of NO^+/O_2^+ at night so the ratios are not shown. The better agreement of Keneshea et al,(1970) at night implies that NO may have a diurnal variation.

THE DISTRIBUTION OF METALLIC IONS

The daytime metallic ion belt observed by rockets 14.425 and 14.424 is illustrated in Figure 2. The metallic ions are contained in a layer which maximizes near 92 km with a density of 400 cm^{-3}. The principal ions are Mg^+ and Fe^+. Smaller concentrations of Na^+, Al^+, K^+, Ca^+ and possibly Si^+ are also observed. Important minor isotopes of the above constituents are observed but not shown. The minor constituents are less apparent in the data of 14.425 because of inferior operating conditions for this instrument. This may also account in part for the apparent depletion in 24^+ below 92 km in this flight.

From the daytime data it is seen that the metallic layers are well defined at the magnetic equator, although of broader peak width than at midlatitudes, (Narcisi and Bailey, 1965; Narcisi, 1968; Young et al, 1967). Above 100 km a low

background of metallics occurs to apogee, with no secondary ledges of metal ions in the 110 km range as observed at midlatitudes.

The nighttime data are illustrated in Figure 3. The height resolution on these flights is poorer because of sampling under conditions of larger velocities. The spectrometer sweep range for the nighttime flights did not exceed 42^+, so that Fe^+ must be approximated by the T_B curve. Although the nighttime estimate of Fe^+ is based on high pass filter mode data which includes an unknown fractional contribution of O_2^+, this does not significantly alter the magnitude of Fe^+ at the lower altitudes (below 102 km on 18.97 and below 97 km on 18.98) where O_2^+ is a trace constituent relative to T_B. Finally, we note that the spectrometer aboard 18.97 had less sensitivity than that aboard 18.98.

The observed metallic belt in the data of 18.97 exhibits a broad maximum centered near 98 km with a peak density near $10^3/cm^3$. The measurement was made at post-sunset, when the F layer had reached an altitude of 550 km as determined from ionogram analysis. The data of 18.98 were obtained after the F layer maximum had drifted downward to 300 km. At this time the metallic layer is observed to be more pronounced, with properties quite similar to the daytime case, but for a peak density over twice as large. There is no evidence for sporadic E on ionograms recorded during either of the two night flights.

Awe (1971) has recently reported that the equatorial sporadic E virtual height ($h'E_s$) exhibits an in-phase correlation with the postsunset drift induced height shift of the equatorial F layer. Typical E_s drift velocities are 1-3 m/sec. The data presented here illustrate that the equatorial metallic layer is subjected to similar drifts, induced by dynamo electric fields. The magnitude of the observed displacement (6 km) can be accounted for by an average downward drift of approximately 1 m/sec between flights.

The height of the nighttime metallic layer coincides with a depletion of NO^+ and O_2^+, an effect most pronounced in the data of 18.98. Similar type depletions at midlatitude have been observed by Narcisi (1968) and he has suggested that charge exchange between NO^+ and neutral metallics is the reason for this effect. In the following sections the theory of the metallic ion distribution will be examined in detail.

DISCUSSION

The temporal variation of the metals depends on several factors including:

1) the distribution of the neutral metals in space and time.

2) ionic reactions as detailed in Table II.

3) ion motion imposed by electric fields, diffusion effects, and other external forces.

a. Photochemistry of the Metals

The reactions and rate coefficients describing the behavior of metals in the upper atmosphere are poorly known. Nevertheless reasonable estimates can be made for most of the important processes. The reactions which have been included in the computations together with the assumed rate coefficients are listed in Table II. For comparison purposes the measured rate coefficient is also given and utilized wherever possible.

The metal ions can be placed into two categories. The first group contains Mg^+, Al^+, Fe^+ and Ca^+. These ions react with O_2 and O_3 to form molecular ions such as XO_2^+ and XO^+ where X is any of the above constituents. Such ions recombine dissociatively with electrons at a much greater rate than would be the case if the ions were atomic. The second group contains alkalai metals such as Na^+ and K^+. There is apparently no molecular ion formation for these ions in a manner akin to the group I ions. However, laboratory observations (Keller and Beyer, 1971 b) have shown that 3 body reactions such as

$$Na^+ + CO_2 + CO_2 \rightarrow Na^+ \cdot CO_2 + CO_2$$

do occur with large rate coefficients.

The present computations do not consider the chemical behavior of the neutral metals. No metallic oxide processes

and no diurnal variation of the neutral metals as the result of either photodissociation of metal oxide compounds or changes in the concentration of minor constituents (as for example, ozone) are considered here. Similarly there has been no attempt to include the diffusion of the neutral metals either from the top of the layer as was done by Hanson and Donaldson (1967) and Gadsden (1970) or as loss out the bottom. In the model, neutral metals are created only through dissociative recombination of molecular metal ions. None of the above processes or values are sufficiently understood or known to warrant inclusion at this time.

The initial altitude distribution of the neutral metals assumed for the model is given in Table III. Little is known about the neutral metal distribution in this region. However, by the use of resonant scattering of a laser beam (Gibson and Sanford 1971) the sodium distribution has been studied. These observations are consistent with determinations from airglow monitoring performed with rockets (Hunten and Wallace, 1967) in that they show a neutral sodium layer centered between 90 and 95 km with a maximum concentration of $10^3/cm^3$. The uncertainties of distribution are even greater for the other remaining metals and most have never been measured. Hunten (1964), Vallance-Jones (1966), and Gadsden (1970) have reviewed the distribution for other metals such as potassium. With the exception of neutral sodium at 93 km, all neutral metallic distributions in Table III are those required to produce the measured ion distribution.

Under the above considerations and restrictions, the computed distribution of metallic ions for daytime conditions is shown in Figure 6. The agreement between theory and experiment is dependent not only on the rate coefficients but also on the assumed concentrations of neutral metals. In this instance the most obvious lack of agreement is between the observed and calculated distribution of Na^+. The number density of Na^+ observed is nearly two orders of magnitude less than that required by Keller and Beyer (1971 b) in suggesting that clustering of Na^+ to CO_2 and O_2 could explain the distribution of Na^+.

The predicted distribution of Mg^+ is in much better agreement with observations. The ratio Mg^+/Mg is 1.8 at 93 km and the total column density for Mg^+ is estimated to be near 2×10^9 cm^{-2}. Anderson and Barth (1971) have shown $Mg^+/Mg \geq 22$ within a sporadic E layer but with a similar Mg^+ column density of 2×10^9 cm^{-2}. Gadsden (1972) has suggested a factor of 20 higher for this quantity. The agreement of our value with Anderson and Barth implies a relatively constant total content for metal ions, which redistributes under the influence of dynamo effects. No significant diurnal variation of the metal ions is predicted (see Figure 7 for Mg^+). Hence, another mechanism must be introduced to compensate for the observed diurnal variablity.

b. Drift

The data indicate that between the first and second nighttime measurement an increase occurred in the metal ions centered at 92 km. The increase was coupled with a sharp decrease in NO^+. The data suggest a downward moving layer

of ions, averaging a speed of order ~ 1 m/s, in phase with ionospheric observations of electron density drift at higher altitudes (Balsley and Woodman, 1969) and equatorial $h'E_s$ (Awe, 1971).

This drift is represented in the model by means of an additional production term in the equations, which forms metallic ions at a particular rate at a given altitude. The inclusion of drift in this emperical manner simplifies the numerical solutions and is equivalent to including the divergence term in the continuity equation, assuming vertical drift to be independent of altitude. The validity of this approach lies in providing results within the scope of data accuracy and does not alter the final conclusions of the work. Because of differences in concentration gradient the term will vary for each metal ion species. The magnitude of the equivalent production term used for each species for a downward velocity of 1 m/sec are based on the measured data. The downward drift is imposed at 1900 hours, continued as a constant until 0240 hours, and then discontinued. This phasing roughly corresponds to the mean nighttime motion of the F region on the night of the rocket flights.

The resulting profile for major constituents at 0100 is shown in Figure 8 for situations with and without drift. It can be seen that the required increase in metal ions occurs coupled by a decrease in NO^+. This

effect is significantly stronger with drift included. In order to enhance NO^+ and reduce Fe^+ and Mg^+ near 90 km as observed, it is necessary to apply a velocity gradient decreasing to zero near 90 km, rather than the simplified uniform drift model used here.

The reason for the decrease in NO^+, when more metal ions are introduced into a region, is the enhancement of the neutral metal density. Figure 7 illustrates the diurnal variation of Mg with and without ion drift. The ion Mg^+ rapidly converts to MgO^+ which in turn recombines with ambient electrons to form Mg. The neutral density is enhanced and remains enhanced as does the metallic ion density. This can be contrasted with the daytime observations, which are characterized by smaller local metal ion densities and no depletion of NO^+. Presumably during daytime, there is an upward drift of the metal ions. This must commence early in the morning and terminate for zenith angles less than 60^o, if the same photochemistry is to be involved to explain the daytime distribution.

The neutral metal concentrations must also decrease during daytime. No processes representing the loss of neutral metals by leakage from the bottom of the layer or chemical reaction to form other compounds have been included hence the results are not fully quantitative. It is clear, however, that any explanation of the behavior of the various

ion species in the lower E layer at the magnetic equator must include the effects of drift. It is also apparent that photochemistry is inadequate to explain the observed behavior of metals at midlatitudes, suggesting that drifts must once again be taken into account.

CONCLUSIONS

Measurements have been carried out of the positive ion species comprising the magnetic equatorial E region during both day and night conditions. In addition to the gaseous ionic species NO^+, O_2^+ and N_2^+, metallic ions are also present. Under daytime conditions, these ions are located in a layer centered at 92 km and of approximate half width - 3 km. The maximum concentration of the primary ion, Mg^+, is 300 ions/cm^3. At higher altitudes the density is of the order of 10/cm^3. No enhanced layers responsible for mid-latitude type sporadic E are observed.

Nighttime data show a variation of metallic ion concentration with time. This suggests a downward motion of metal ions in the E region. By transformation of metal atomic ions into metal oxide ions at lower altitudes, the ion-electron recombination rate can be enhanced. The dissociative recombination of metal ions then enhances the neutral metal concentration, so that charge exchange between neutral metals and NO^+ and O_2^+ depletes the population of NO^+ and O_2^+. A velocity of 1 m/sec operating for 6 hours is sufficient to reproduce the observations. Nighttime light metal ion (Na^+, Mg^+)

densities above 100 km are nearly constant and of order $10/cm^3$ to nearly 300 km. The density of Fe^+ most certainly does not exceed this value above 100 km.

Unfortunately, the current reaction schemes are inadequate to account for the apparent depletion of alkalai metal ions, Na^+ and K^+. Our knowledge concerning neutral sodium predicts Na^+ to exist in much larger quantities than observed.

Reaction rates for neutral and metallic ions are still poorly defined. Much laboratory and in situ rocket investigation is needed before a quantative description of the metallic ion distribution will be possible (especially for the alkalai metals). Future experiments should measure the ion and neutral metal altitude distribution simultaneously on a diurnal basis to resolve the gaps in our understanding of the metallic E region structure. In addition, the apparent difficulty in obtaining sufficient production sources to produce the NO^+ and O_2^+ distributions must be resolved. Only then will the E region be satisfactorily understood and provide useful input for the ionospheric models.

ACKNOWLEDGEMENT

This program was successfully completed through the diligent efforts of the technical staff assigned to the Chemosphere Branch for direct support of this work. In particular, we thank Mr. Donald Silbert for his contributions to the technical development of the quadrupole ion mass spectrometer and associated systems for application to this work. Messrs. Roy Hagemeyer and Giles Spaid were largely responsible for the radio wave absorption experiment. Mr. P.D. Smidinger performed most of the tedius numerical analysis. We thank members of the Goddard Sounding Rocket Division for the many services they performed including introduction of tone ranging to determine trajectory. The assistance of Mr. John Jackson in the analysis of the CW propagation electron density profile and in the trajectory analysis is greatly appreciated. We also thank the Indian Launch Range (TERLS) under the directorship of Mr. H.G.S. Murthy, for their excellent cooperation and support.

REFERENCES

Aikin, A. C. and L.J. Blumle, "Rocket Measurements of the E Region Electron Concentration Distribution in the Vicinity of the Geomagnetic Equator", J. Geophys. Res., 73, 1617, 1968.

Aikin, A. C., R. A. Goldberg, Y.V. Somayajulu and M.B. Avadhanulu, "Electron and Positive Ion Density Altitude Distributions in the Equatorial D Region", J. Atmos. Terr. Phys., (in press).

Anderson, J.G. and C.A. Barth, "Rocket Investigations of the MgI and MgII Dayglow", J. Geophys. Res., 76, 3723, 1971.

Argo, H.V., J.A. Bergey and W.D. Evans, "Measurements of the Solar X-Ray Flux in Selected Emission Lines", Astrophys. J., 160, 283, 1970.

Awe, O., "Studies of Nighttime E_s at Ibadan Near the Magnetic Equator", J. Atmos. Terr. Phys., 33, 1209, 1971.

Balsley, B.B., "Nighttime Electric Fields and Vertical Ionospheric Drifts near the Magnetic Equator", J. Geophys. Res., 74, 1213, 1969a.

Balsley, B.B., "Measurement of Electron Drift Velocities in the Nighttime Equatorial Electrojet", J. Atmos. Terr. Phys., 31, 475, 1969b.

Balsley, B.B. and R.F. Woodman, "On the Control of the F-Region Drift Velocity by the E Region Electric Field: Experimental Evidence", J. Atmos. Terr. Phys., 31, 865, 1969.

Bates, D.R. and A. Dalgarno, "Electric Recombination", Atomic and Molecular Processes (D.R. Bates, ed.), Academic Press, New York, 245, 1962.

Bauer, S.J. and J.E. Jackson, "Rocket Measurements of the Upper Atmosphere by a Radio Propagation Technique", J. Brit. IRE, 23, 139, 1962.

Bourdeau, R.E., A.C. Aikin and J.L. Donley, "Lower Ionosphere at Solar Minimum", J. Geophys. Res., 71, 727, 1966.

Chimonas, G. and I.W. Axford, "Vertical Movement of Temperate-Zone Sporadic E Layers", J. Geophys. Res., 73, 111, 1968.

Danilov, A.D., "Ion Composition and Photochemistry of the E-Region", Proceedings COSPAR Symposium on D- and E-Region Chemistry, Urbana, Ill., 1972.

Farragher, A.L., J.A. Pedin and W.L. Fite, "Charge Transfer of N_2^+, O_2^+, and NO^+ to Sodium Atoms at Thermal Energies", J. Chem. Phys., 50, 287, 1969.

Ferguson, E.E. and F.C. Fehsenfeld, "Some Aspects of the Metal Ion Chemistry of the Earth's Atmosphere", J. Geophys. Res., 73, 6215, 1968.

Ferguson, E.E., "Atmospheric Metal Ion Chemistry", Radio Science, 7, 397, 1972.

Gadsden, M., "Metallic Atoms and Ions in the Upper Atmosphere", Ann. Geophys., 26, 141, 1970.

Gadsden, M., "Dayglow of MgI and MgII", J. Geophys. Res., 77, 1330, 1972.

Gibson, A.J. and M.C.W. Sandford, "The Seasonal Variation of the Night-time Sodium Layer", J. Atmos. Terr. Phys., 33, 1675, 1971.

Goldberg, R.A. and L.J. Blumle, "Positive Ion Composition from a Rocket-Borne Mass Spectrometer", J. Geophys. Res., 75, 133, 1970.

Goldberg, R.A. and A.C. Aikin, "Studies of Positive Ion Composition in the Equatorial D Region Ionosphere", J. Geophys. Res., 76, 8352, 1971.

Hanson, W.B. and J.S. Donaldson, "Sodium Distribution in the Upper Atmosphere", J. Geophys. Res., 72, 5513, 1967.

Hudgins, J.I. and J.R. Lease, "Tone Range-Telemetry Tracking System for Support of Sounding Rocket Payload", NASA SP-219, 187, 1969.

Hunten, D.M., "Metallic Emissions from the Upper Atmosphere", Science, 145, 26, 1964.

Hunten, D.M. and L. Wallace, "Rocket Measurements of the Sodium Dayglow", J. Geophys. Res., 72, 69, 1967.

Istomin, V.G., "Ions of Extra-Terrestrial Origin in the Earth's Ionosphere", Space Research, III, 209, 1963.

Jackson, J.E., "The P'(f) to N(h) Inversion Problem in Ionospheric Studies", NASA X-625-71-154, Goddard Space Flight Center, Greenbelt, Md., 1971.

Keller, G.E. and R.A. Beyer, "Drift Tube Studies of Carbon Dioxide Clustering to Potassium and Sodium Ions", Bull. Am. Phys. Soc., 16, 214, 1971a.

Keller, G.E. and R.A. Beyer, "CO and O_2 Clustering of Sodium Ions", J. Geophys. Res., 76, 289, 1971b.

Keneshea, T.J., "A Technique for Solving the General Reaction-Rate Equations in the Atmosphere", Air Force Cambridge Research Laboratories Report No. AFCRL-67-0221, 1967.

Keneshea, T.J., R.S. Narcisi and W. Swider,Jr., "Diurnal Model of the E Region", J. Geophys. Res., 75, 845, 1970.

Manson, J.E., "The Spectrum of the Quiet Sun between 30 and 128A for November, 1965", Astrophys. J., 147, 703, 1967.

Maynard, N.C. and L.J. Cahill, Jr., "Measurement of the Equatorial Electrojet over India", J. Geophys. Res., 70, 5923, 1965.

Meira, L.G., Jr., "Rocket Measurements of Upper Atmospheric Nitric Oxide and Their Consequence to the Lower Ionosphere", J. Geophys. Res., 76, 202, 1971.

Narcisi, R.S. and A.D. Bailey, "Mass Spectrometric Measurements of Positive Ions at Altitudes from 64 to 112 Kilometers", J. Geophys. Res., 70, 3687, 1965.

Narcisi, R.S., "Processes Associated with Metal-Ion Layers in the E Region of the Ionosphere", Space Research, VIII, 360, 1968.

Rol, P.K. and E.A. Entemann, "NaO^+ Production from Na and O_2^+ in Merged Beams", J. Chem. Phys., 49, 1430, 1968.

Rutherford, J.A., R.G. Mathis, B.R. Turner and D.A. Vroom, "Formation of Magnesium Ions by Charge Transfer", J. Chem. Phys., 55, 3785, 1971.

Seddon, J.C., "Propagation Measurements in the Ionosphere with the Aid of Rockets", J. Geophys. Res., 58, 323, 1953.

Swider, W. Jr., "Processes for Meteoritic Elements in the E Region", Planet. Space Sci., 17, 1233, 1969.

Vallance-Jones, A., "Abundance of Metallic Atoms in the Atmosphere", Ann. Geophys., 22, 189, 1966.

Whitehead, J.D., "Formation of Sporadic E Layer in the Temperate Zone", J. Atmos. Terr. Phys., 20, 49, 1961.

Young, J.M., C.Y. Johnson and J.C. Holmes, "Positive Ion Composition of a Temperate-Latitude Sporadic E Layer as Observed During a Rocket Flight", J. Geophys. Res., 72, 1473, 1967.

LIST OF TABLES

TABLE I

Parameter	18.97	18.98	14.425	14.424
Rocket Type	Nike-Tomahawk		Nike-Apache	
Date (1970)	March 9	March 10	March 19	March 19
Launch Time (LMT)	1938	0108	0827	1017
Solar Zenith Angle			53.2°	27.8°
Payload Weight (lb)	155	155	137	130
Spin Rate (c/s)	6.3	5.6	5.9	7.9
Coning Angle	±4°	±4°	< ±10°	< ±1°
Coning Period (sec)	4	4	2.8	1.0
Trajectory Azimuth (Clockwise from North)	226°	210°	267°	259°
Payload Aspect Azimuth	226° *	210° *	275°	256.3°
Elevation	85°	86°	71.4°	72.9°
Apogee Altitude (km)	298.0	295.1	100.8	121.9
Range Location				
Latitude	8.53°N			
Longitude	76.95°E			
Magnetic Dip	-1.7°			

* Azimuth assumed to lie in the trajectory plane.

TABLE II a

Reaction	Rate Employed	Laboratory Value	Reference
$Al+h\nu \rightarrow Al^+ + e$	4(-4)	4.0(-4)	Swider (1969)
$Al^+ + O_2 + N_2 \rightarrow AlO_2^+ + N_2$	1(-30)		
$Al^+ + O_3 \rightarrow AlO^+ + O_2$	1.5(-10)		
$AlO_2^+ + O \rightarrow AlO^+ + O_2$	1(-10)		
$O_2^+ + Al \rightarrow AlO^+ + O$	1(-11)		
$O_2^+ + Al \rightarrow Al^+ + O_2$	1(-10)		
$NO^+ + Al \rightarrow AlO^+ + N$	1(-11)		
$NO^+ + Al \rightarrow Al^+ + NO$	1(-10)		
$AlO^+ + O \rightarrow Al^+ + O_2$	1(-10)		
$Al^+ + e \rightarrow Al+h\nu$	1(-12)	1(-12)	Bates and Dalgerno (1962)
$AlO^+ + e \rightarrow Al+O$	5(-7)		
$AlO_2^+ + e \rightarrow Al+O_2$	5(-7)		
$N_2^+ + Al \rightarrow Al^+ + N_2$	1(-10)		

TABLE II b

Reaction	Rate Employed	Laboratory Value	Reference
$Ca+h\nu \rightarrow Ca^{+}+e$	3.5(-5)	3.5(-5)	Swider (1969)
$Ca^{+}+O_2+N_2 \rightarrow CaO_2^{+}+N_2$	6.6(-30)	~6.6(-30)*	Ferguson and Fehsenfeld (1968)
$Ca^{+}+O_3 \rightarrow CaO^{+}+O_2$	1.6(-10)	1.6(-10)	Ferguson and Fehsenfeld (1968)
$CaO_2^{+}+O \rightarrow CaO^{+}+O_2$	1(-10)		
$O_2^{+}+Ca \rightarrow CaO^{+}+O$	1(-11)		
$O_2^{+}+Ca \rightarrow Ca^{+}+O_2$	1(-10)	4.1(-9)**	Rutherford et al (1971)
$NO^{+}+Ca \rightarrow CaO^{+}+N$	1(-11)		
$NO^{+}+Ca \rightarrow Ca^{+}+NO$	1(-10)	4.0(-9)**	Rutherford et al (1971)
$CaO^{+}+O \rightarrow Ca^{+}+O_2$	1(-10)		
$Ca^{+}+e \rightarrow Ca+h\nu$	1(-12)	~1(-12)	Bates and Dalgarno (1962)
$CaO^{+}+e \rightarrow Ca+O$	5(-7)		
$CaO_2^{+}+e \rightarrow Ca+O_2$	5(-7)		
$N_2^{+}+Ca \rightarrow Ca^{+}+N_2$	5(-10)	1.7(-9)**	Rutherford et al (1971)

* Third body is Ar

** Thermal energy estimate by Ferguson (1972).

TABLE II c

Reaction	Rate Employed	Laboratory Value	Reference
$Fe+h\nu \rightarrow Fe^{+}+e$	5(-7)	5(-7)	Swider (1969)
$Fe^{+}+O_2+N_2 \rightarrow FeO_2^{+}+N_2$	1(-30)	~1.0(-30)	Ferguson and Fehsenfeld (1968)
$Fe^{+}+O_3 \rightarrow FeO^{+}+O_2$	1.5(-10)	1.5(-10)	Ferguson and Fehsenfeld (1968)
$FeO_2^{+}+O \rightarrow FeO^{+}+O_2$	1(-10)		
$O_2^{+}+Fe \rightarrow FeO^{+}+O$	1(-11)		
$O_2^{+}+Fe \rightarrow Fe^{+}+O_2$	1(-10)	1.2(-9)**	Rutherford et al (1971)
$NO^{+}+Fe \rightarrow FeO^{+}+N$	1(-11)		
$NO^{+}+Fe \rightarrow Fe^{+}+NO$	1(-10)	9.1(-10)**	Rutherford et al (1971)
$FeO^{+}+O \rightarrow Fe^{+}+O_2$	1(-10)		
$Fe^{+}+e \rightarrow Fe+h\nu$	1(-12)	~1(-12)	Bates and Dalgarno (1962)
$FeO^{+}+e \rightarrow Fe+O$	5(-7)		
$FeO_2^{+}+e \rightarrow Fe+O_2$	5(-7)		
$N_2^{+}+Fe \rightarrow Fe^{+}+N_2$	5(-10)	4.3(-10)**	Rutherford et al (1971)

** Based on extrapolation to thermal energies by Ferguson (1972)

TABLE II d

Reaction	Rate Employed	Laboratory Value	Reference
$K+h\nu \rightarrow K^+ + e$	2.9(-5)	2.9(-5)	Swider (1969)
$K+2O_2 \rightarrow K^+ \cdot O_2 + O_2$	2.5(-33)	<2(-31)	Ferguson and Fehsenfeld (1968)
$K^+ \cdot O_2 + O_2 \rightarrow K^+ + 2O_2$	2.5(-13)		
$K^+ + CO_2 + CO_2 \rightarrow K^+ \cdot CO_2 + CO_2$	4.0(-30)	1.0(-29)*	Keller and Beyer (1971 a)
$K^+ \cdot CO_2 + CO_2 \rightarrow K^+ + 2CO_2$	2(-13)	5(-14)*	Keller and Beyer (1971 a)
$K^+ + 2N_2 \rightarrow K^+ \cdot N_2 + N_2$	2.5(-30)		
$K^+ \cdot N_2 + N_2 \rightarrow K^+ + 2N_2$	2.5(-13)		
$O_2^+ + K \rightarrow KO^+ + O$	7.7(-11)		
$NO^+ + K \rightarrow KO^+ + N$	7.7(-11)		
$NO^+ + K \rightarrow K^+ + NO$	1(-10)		
$O_2^+ + K \rightarrow K^+ + O_2$	1(-10)		
$KO^+ + e \rightarrow K + O$	5(-6)300/T		
$K^+ \cdot O_2 + e \rightarrow K + O_2$	5(-6)300/T		
$K^+ \cdot N_2 + e \rightarrow K + N_2$	5(-6)300/T		
$K^+ \cdot CO_2 + e \rightarrow K + CO_2$	5(-6)300/T		
$K^+ + e \rightarrow K + h\nu$	1(-12)	~1(-12)	Bates and Dalgarno (1962)
$N_2^+ + K \rightarrow K^+ + N_2$	1(-10)		

* Value at 193° K

TABLE II e

Reaction	Rate Employed	Laboratory Value	Reference
$Mg+h\nu \rightarrow Mg^+ + e$	$4x10^{-7}$ sec^{-1}	4(-7)	Swider (1969)
$Mg^+ + O_2 + M \rightarrow MgO_2^+ + M$	$2.5x10^{-30}$	2.5(-30)	Ferguson and Fehsenfeld (1968)
$Mg^+ + O_3 \rightarrow MgO^+ + O_2$	$2.3x10^{-10}$	2.3(-10)	Ferguson and Fehsenfeld (1968)
$MgO_2^+ + O \rightarrow MgO^+ + O_2$	$1.0x10^{-10}$		
$O_2^+ + Mg \rightarrow MgO^+ + O$	1(-11)		
$O_2^+ + Mg \rightarrow Mg^+ + O_2$	1(-10)	1.2(-10)**	Rutherford et al (1971)
$NO^+ + Mg \rightarrow MgO^+ + N$	1(-11)		
$NO^+ + Mg \rightarrow Mg^+ + NO$	1(-10)	1.0(-9)**	Rutherford et al (1971
$MgO^+ + O \rightarrow Mg^+ + O_2$	1(-10)	1(-10)	Ferguson and Fehsenfeld (1968)
$Mg^+ + e \rightarrow Mg+h\nu$	1(-12)	~1(-12)	Bates and Dalgarno (1962)
$MgO^+ + e \rightarrow Mg+O$	5(-7)		
$MgO_2^+ + e \rightarrow Mg+O_2$	3(-7)		
$N_2^+ + Mg \rightarrow Mg^+ + N_2$	5(-10)		

** Based on extrapolation to thermal energy by Ferguson (1972)

TABLE II f

Reaction	Rate Employed	Laboratory Value	Reference
$Na+h\nu \rightarrow Na^+ + e$	1.7(-5)	1.7(-5)	Swider (1969)
$Na^+ + O_2 + O_2 \rightarrow Na^+ \cdot O_2 + O_2$	1(-31)	1(-31)*	Keller and Beyer (1971 b)
$Na^+ \cdot O_2 + O_2 \rightarrow Na^+ + 2O_2$	4(-13)	4(-13)*	Keller and Beyer (1971 b)
$Na^+ + CO_2 + CO_2 \rightarrow Na^+ \cdot CO_2 + CO_2$	4(-29)	4(-29)*	Keller and Beyer (1971 b)
$Na^+ \cdot CO_2 + CO_2 \rightarrow NA^+ + 2CO_2$	5(-15)	5(-15)*	Keller and Beyer (1971 b)
$Na^+ + N_2 + N_2 \rightarrow Na^+ \cdot N_2 + N_2$	1(-29)		
$Na^+ \cdot N_2 + N_2 \rightarrow Na^+ + 2N_2$	4(-13)		
$Na^+ \cdot CO_2 + e \rightarrow Na + CO_2$	5(-6)300/T		
$Na^+ \cdot O_2 + e \rightarrow Na + O_2$	5(-6)300/T		
$Na^+ \cdot N_2 + e \rightarrow Na + N_2$	5(-6)300/T		
$Na^+ + e \rightarrow Na + h\nu$	1(-12)	~(-12)	Bates and Dalgarno (1962)
$NaO^+ + e \rightarrow NaO + h\nu$	5(-7)		
$NO^+ + Na \rightarrow Na^+ + NO$	7.7(-11)	7.7(-11)	Farragher et al (1969)
$O_2^+ + Na \rightarrow Na^+ + O_2$	6.7(-10)	6.7(-10)	Farragher et al (1969)
		1.4(-9)**	Rutherford et al (1971)
$N_2^+ + Na \rightarrow Na^+ + N_2$	6.7(-10)	7.7(-10)	Farragher et al (1969)
		1.9(-9)**	Rutherford et al (1971)
$O_2^+ + Na \rightarrow NaO^+ + O$	7.7(-11)	7.7(-11)	Rol and Entemann (1968)
$NO^+ + Na \rightarrow NaO^+ + N$	7.7(-11)		

* Value at 193°K
** Based on extrapolation to thermal energies by Ferguson (1972)

TABLE III

ALTITUDE (km)	Neutral Metal Concentration (cm^{-3})					
	Mg	Fe	Na	K	Ca	Al
90	4	77	20	18	8	10
91	320	45	30	16	8	11
93	1000	250	1000	10	10	10
95	60	164	184	7	3	16
100	10	3	10	1	1	1

LIST OF FIGURES

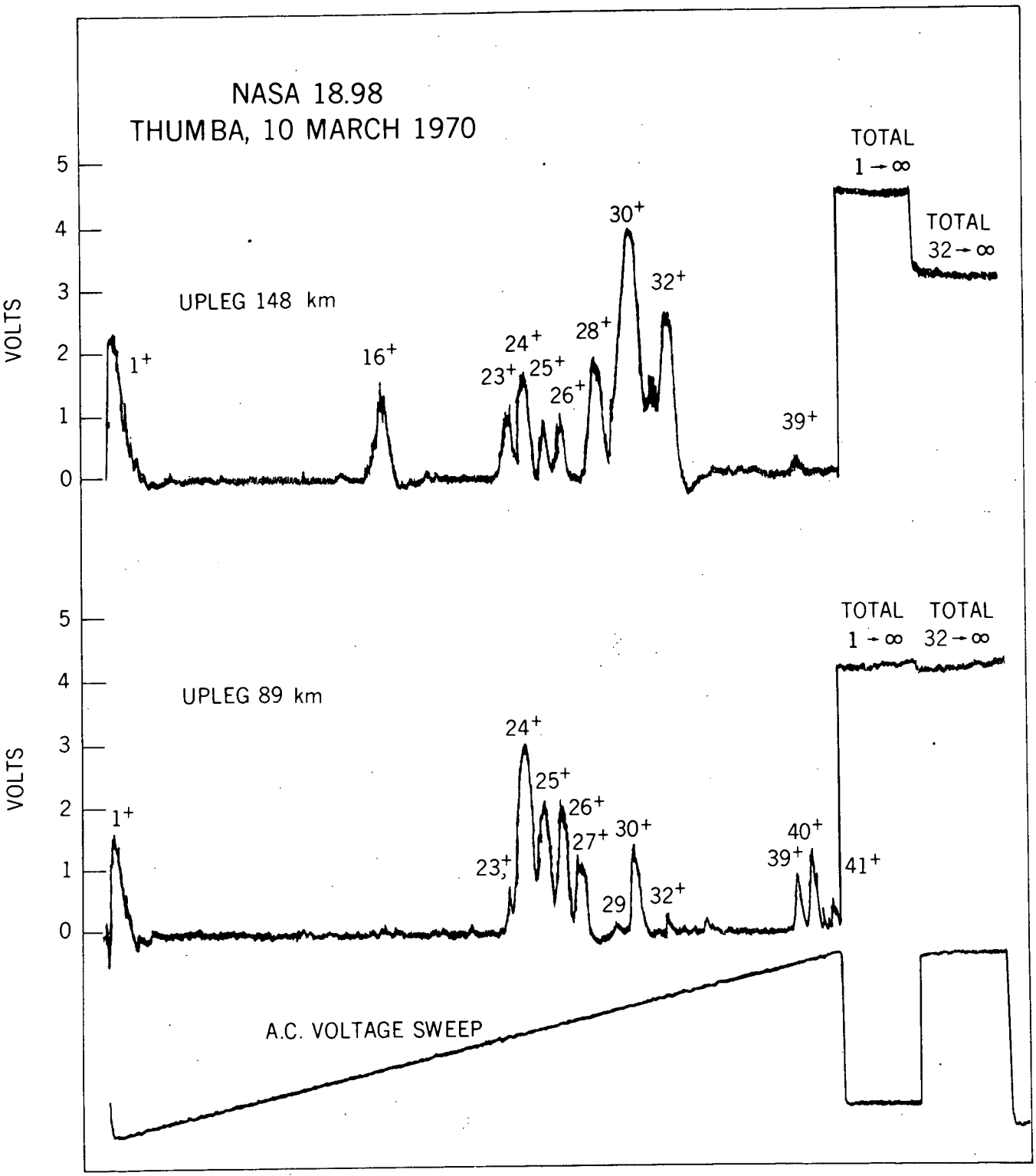
NASA 18.98
THUMBA, 10 MARCH 1970
VOLTS
5
4
3
2
1
0
UPLEG 148 km
TOTAL
1 → ∞
TOTAL
32 → ∞
1+
16+
23+
24+
25+
26+
28+
30+
32+
39+
UPLEG 89 km
TOTAL
1 → ∞
TOTAL
32 → ∞
1+
23+
24+
25+
26+
27+
29
30+
32+
39+
40+
41+
A.C. VOLTAGE SWEEP

Figure 1

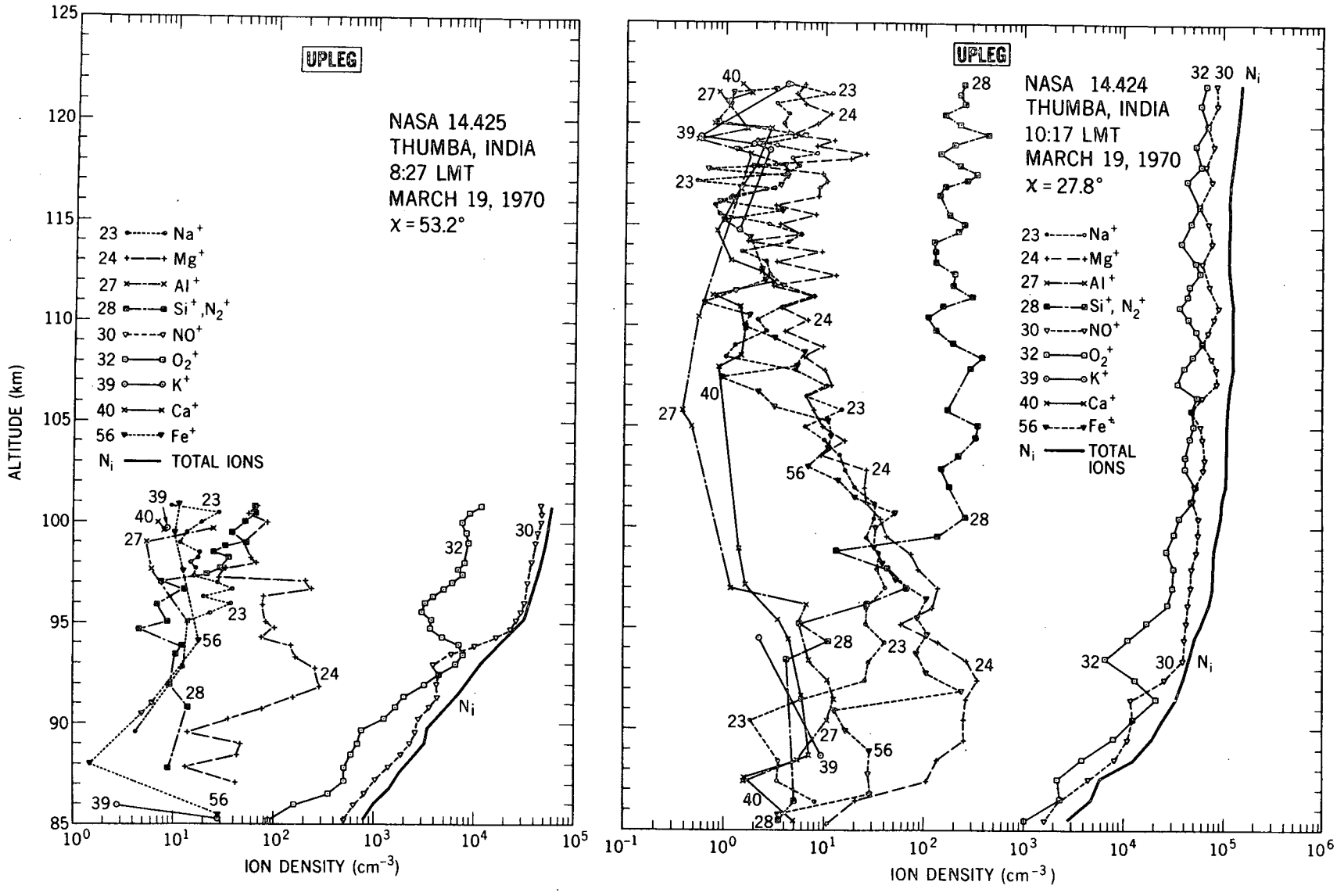
UPLEG
NASA 14.425
THUMBA, INDIA
8:27 LMT
MARCH 19, 1970
χ = 53.2°
23 Na+
24 Mg+
27 Al+
28 Si+, N2+
30 NO+
32 O2+
39 K+
40 Ca+
56 Fe+
Ni TOTAL IONS
ALTITUDE (km)
ION DENSITY (cm-3)
UPLEG
NASA 14.424
THUMBA, INDIA
10:17 LMT
MARCH 19, 1970
χ = 27.8°
23 Na+
24 Mg+
27 Al+
28 Si+, N2+
30 NO+
32 O2+
39 K+
40 Ca+
56 Fe+
Ni TOTAL IONS
ION DENSITY (cm-3)

Figure 2

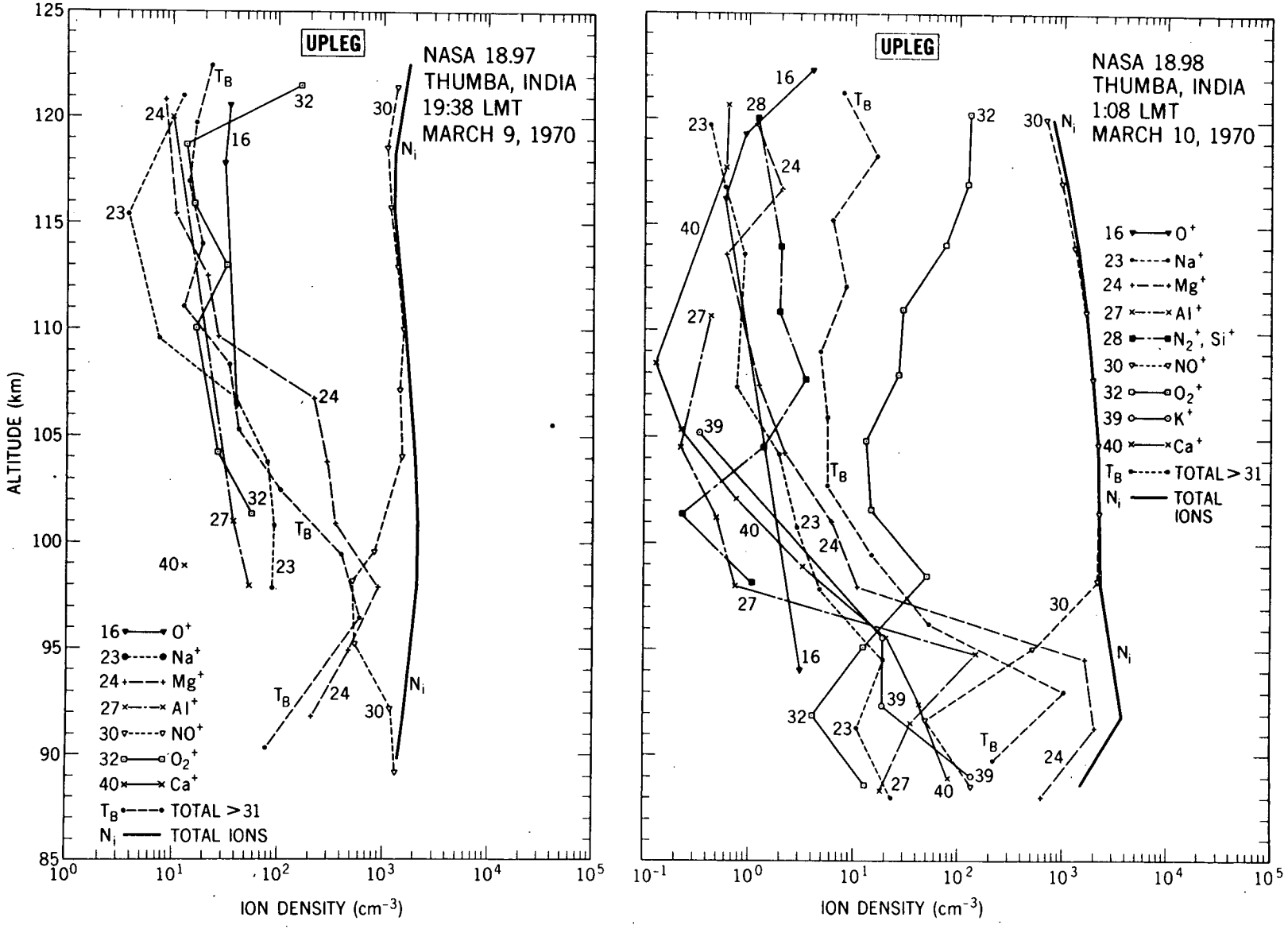
UPLEG
NASA 18.97
THUMBA, INDIA
19:38 LMT
MARCH 9, 1970
ALTITUDE (km)
ION DENSITY (cm^{-3})
16 O$^+$
23 Na$^+$
24 Mg$^+$
27 Al$^+$
30 NO$^+$
32 O$_2^+$
40 Ca$^+$
T$_B$ TOTAL >31
N$_i$ TOTAL IONS
UPLEG
NASA 18.98
THUMBA, INDIA
1:08 LMT
MARCH 10, 1970
ION DENSITY (cm^{-3})
16 O$^+$
23 Na$^+$
24 Mg$^+$
27 Al$^+$
28 N$_2^+$, Si$^+$
30 NO$^+$
32 O$_2^+$
39 K$^+$
40 Ca$^+$
T$_B$ TOTAL > 31
N$_i$ TOTAL IONS

Figure 3

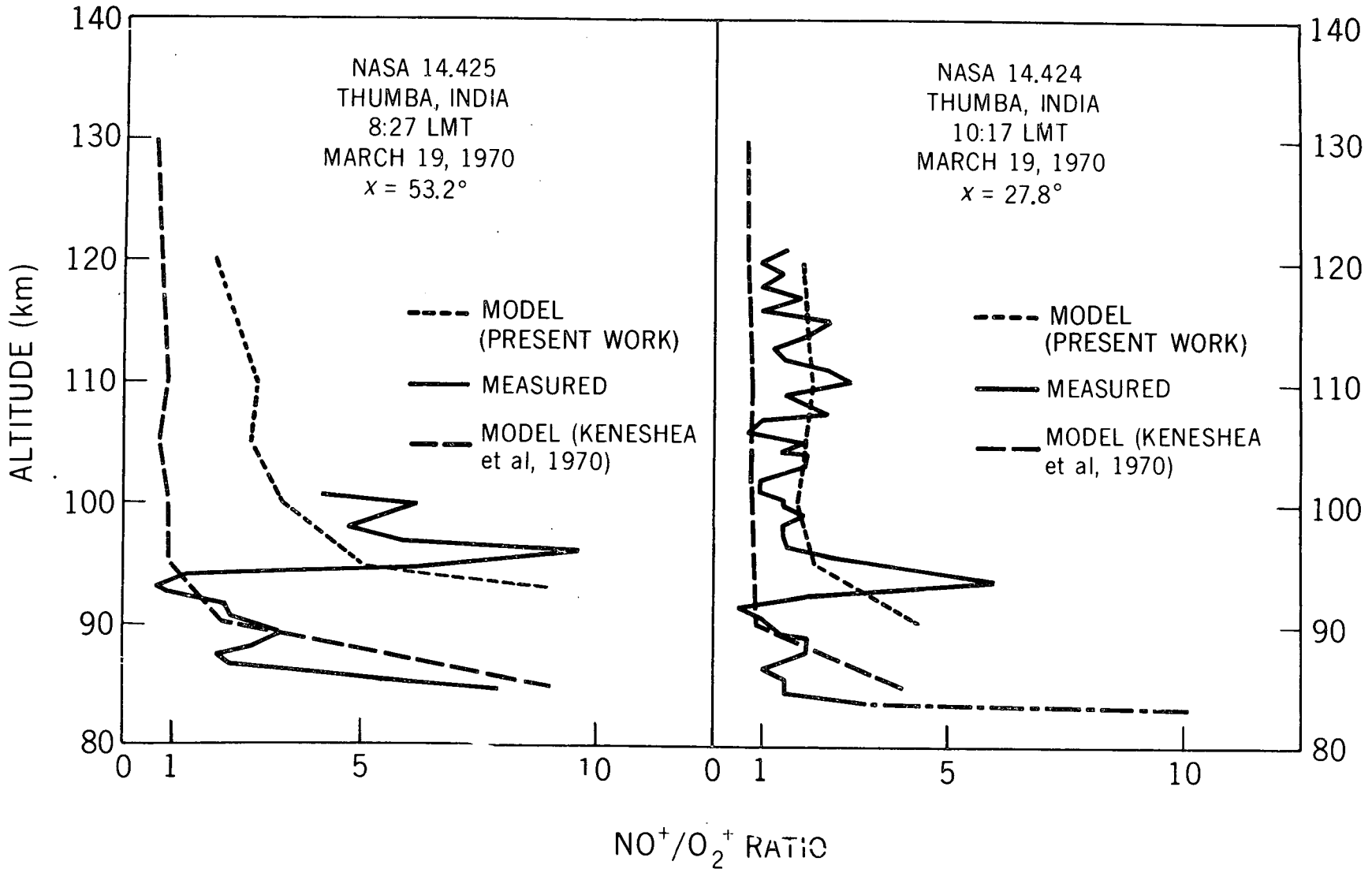
NASA 14.425
THUMBA, INDIA
8:27 LMT
MARCH 19, 1970
x = 53.2°
MODEL
(PRESENT WORK)
MEASURED
MODEL (KENESHEA
et al, 1970)
NASA 14.424
THUMBA, INDIA
10:17 LMT
MARCH 19, 1970
x = 27.8°
MODEL
(PRESENT WORK)
MEASURED
MODEL (KENESHEA
et al, 1970)
ALTITUDE (km)
140
130
120
110
100
90
80
0
1
5
10
NO+/O2+ RATIO

Figure 4

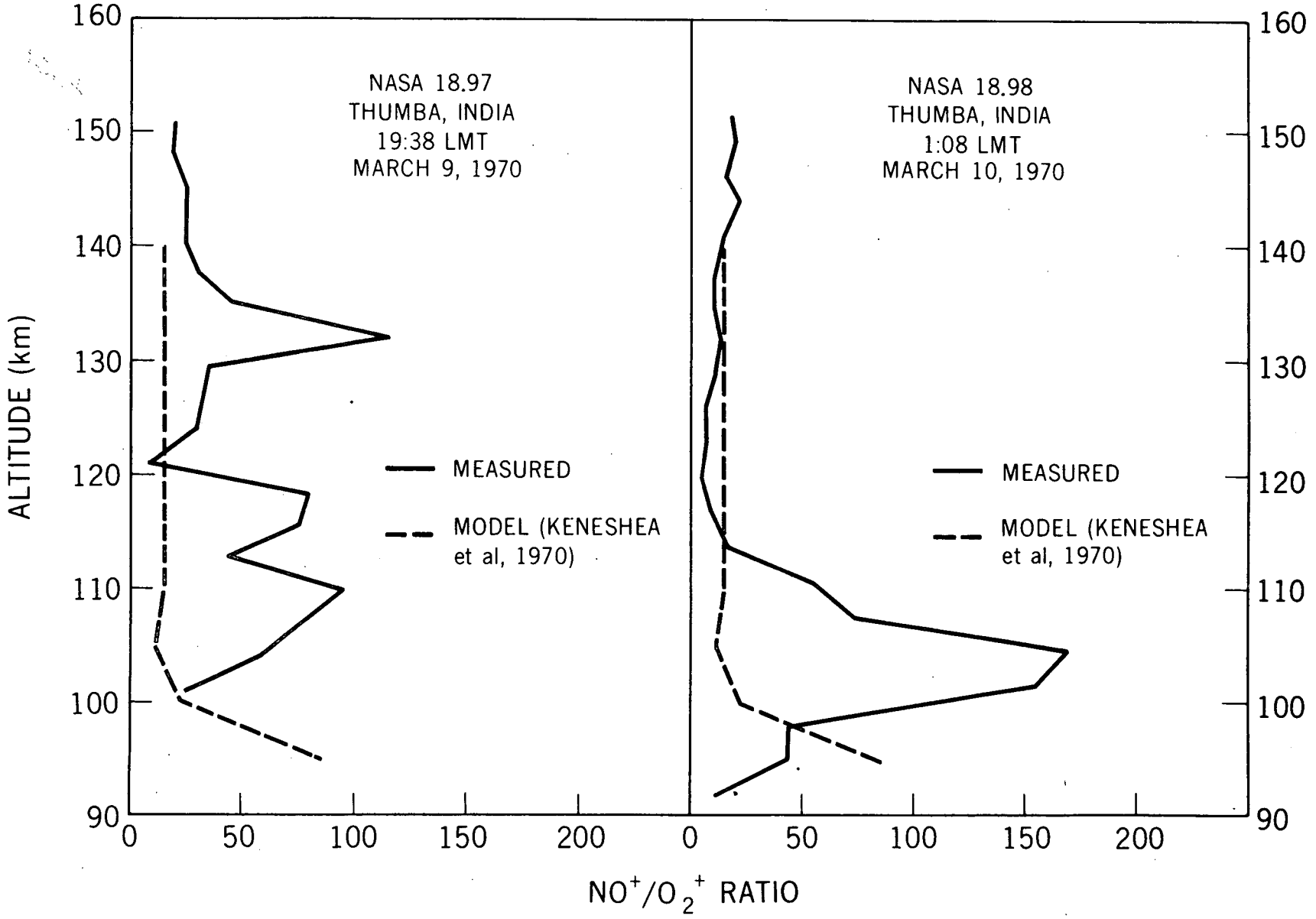
NASA 18.97
THUMBA, INDIA
19:38 LMT
MARCH 9, 1970
NASA 18.98
THUMBA, INDIA
1:08 LMT
MARCH 10, 1970
MEASURED
MODEL (KENESHEA et al, 1970)
MEASURED
MODEL (KENESHEA et al, 1970)
ALTITUDE (km)
160
150
140
130
120
110
100
90
0
50
100
150
200
NO^+/O_2^+ RATIO

Figure 5

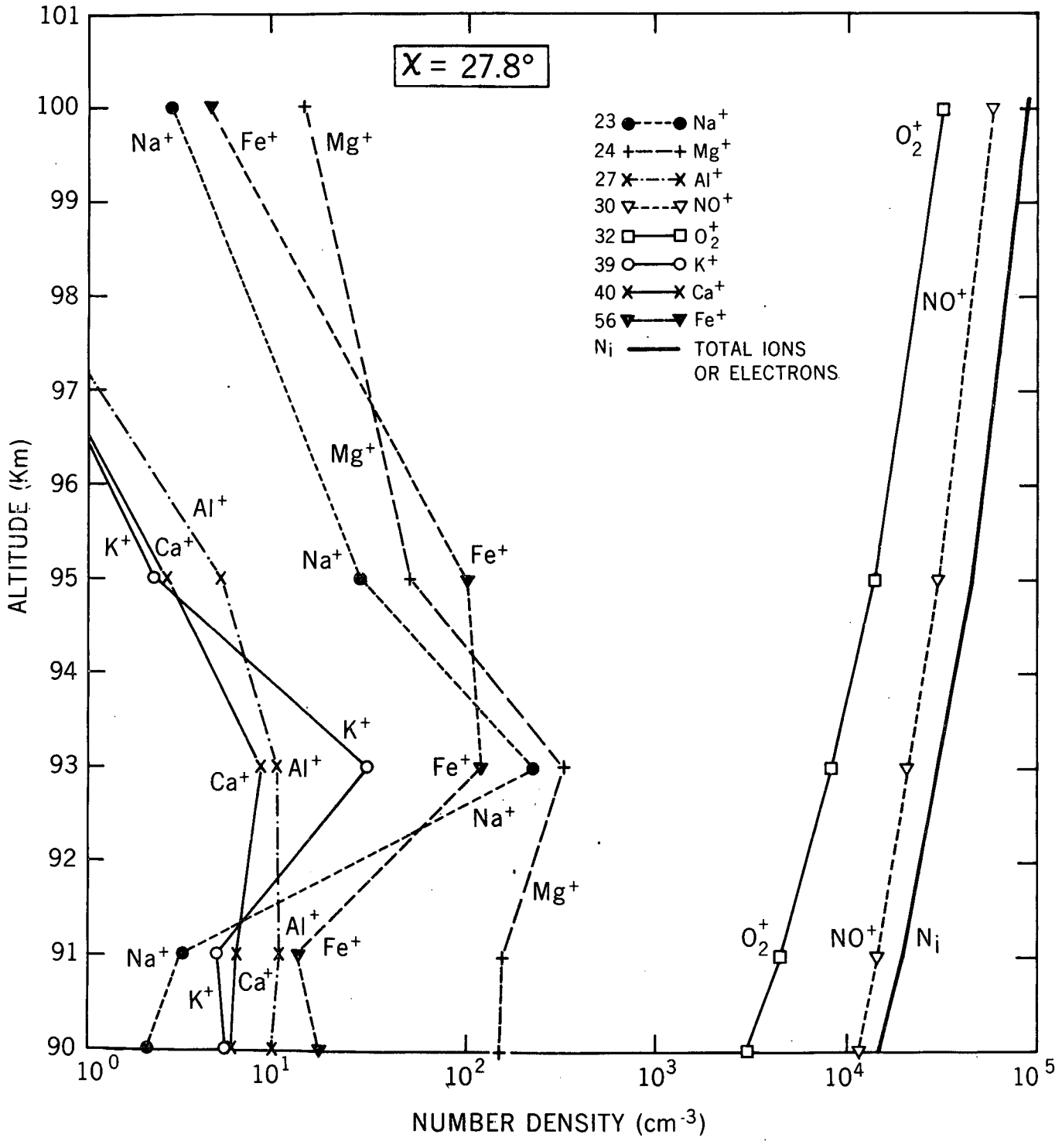
χ = 27.8°
23 Na+
24 Mg+
27 Al+
30 NO+
32 O2+
39 K+
40 Ca+
56 Fe+
Ni TOTAL IONS OR ELECTRONS
ALTITUDE (Km)
NUMBER DENSITY (cm-3)
101
100
99
98
97
96
95
94
93
92
91
90
10 0
10 1
10 2
10 3
10 4
10 5
Na+
Fe+
Mg+
Al+
K+
Ca+
O2+
NO+
Ni

Figure 6

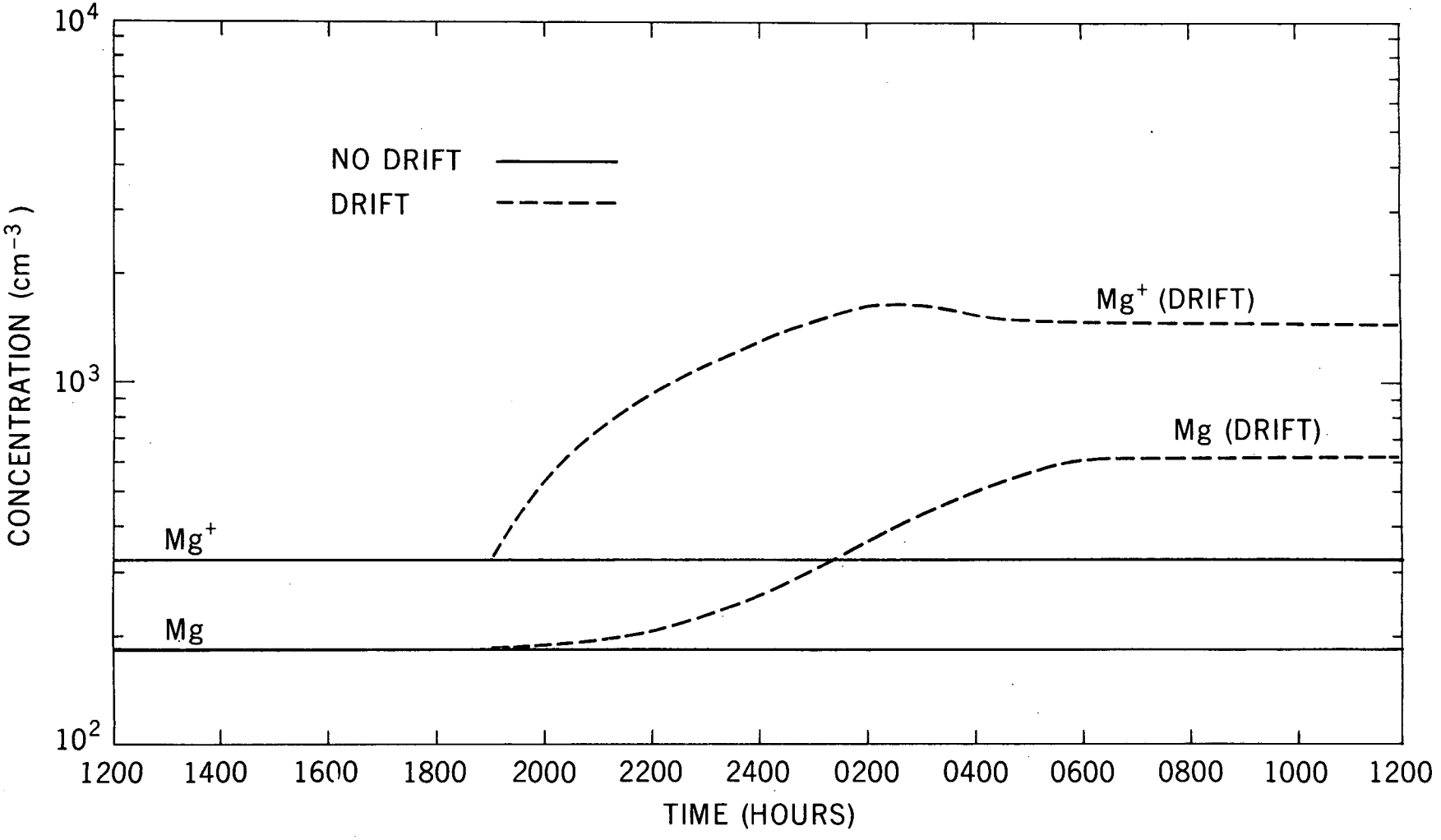
10^4
10^3
10^2
CONCENTRATION (cm^{-3})
NO DRIFT
DRIFT
Mg^+ (DRIFT)
Mg (DRIFT)
Mg^+
Mg
1200
1400
1600
1800
2000
2200
2400
0200
0400
0600
0800
1000
1200
TIME (HOURS)

Figure 7

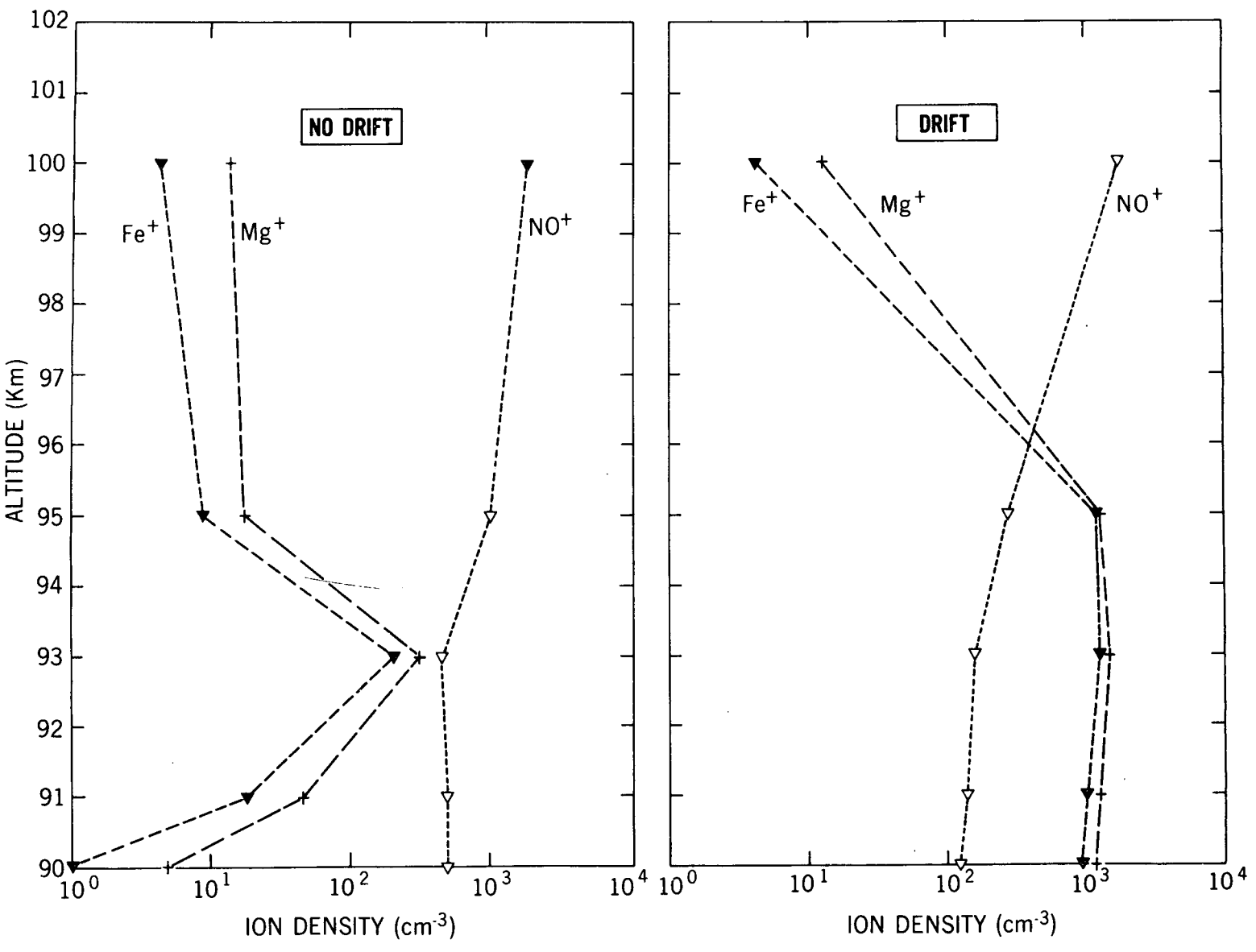
MODEL CALCULATION - 1:00 LMT
NO DRIFT
DRIFT
Fe+
Mg+
NO+
ALTITUDE (Km)
ION DENSITY (cm-3)
102
101
100
99
98
97
96
95
94
93
92
91
90
10 0
10 1
10 2
10 3
10 4
NASA–GSFC

Figure 8